OPEN ACCESS

SCICELL

RESEARCH PAPER

Analysis of the compositions of manganese ores and charges for the production of agglomerate from the position of phase structure diagrams of manganese-containing systems

Ablay Zhunusov[1]*, Sailaubay Baisanov[2], Yerzhan Abdulabekov[3], Petr Bykov[1], Aigul Zhunusova[1], Altynsary Bakirov[1], Anar Kenzhebekova[1]

[1]Toraighyrov University, Lomov 64, Pavlodar city, Kazakhstan
[2]Zh.Abishev Chemical-metallurgical institute, Ermekov 63, Karaganda city, Kazakhstan
[3]Aktobe ferroalloys plant, M. Mametova 4A, Aktobe city, Kazakhstan

*Corresponding author: zhunusov_ab@mail.ru, tel.: +7 747 808 6235, Toraighyrov University, Lomov 64, Pavlodar city, Kazakhstan

ABSTRACT

This paper studies the phase formation processes during the agglomeration of manganese ores of the "Tur" deposit. When introducing dolomite into the composition of the agglomeration batch from the position of thermodynamic-diagram analysis $MgO-MnO-CaO-Al_2O_3-SiO_2$, it is shown that the phase composition of the substance's changes in a certain sequence with entry into one or another pentatope and depends on the completeness of the interaction of dolomite with manganese ore. Adding dolomite to the agglomeration batch leads to the formation of refractory compounds due to the latter's interaction with low-melting manganese compounds. The most low-melting compound in the spessartite system (t_{melt}=1205 ºC), present in the screenings of manganese ores, when interacting with dolomite, will form more refractory compounds of forsterite Mg_2S (t_{melt}=1860 ºC) and diopside CMS_2 (t_{melt}=1391.5 ºC). As a result, the addition of dolomite to the sinter batch of more than 8.4% leads to the transition of the agglomerate composition from pentatope No. 4 ($M_3AS_3-CAS_2-M_2S-Mg_2S-S$) to pentatope No. 3 ($CMS_2-CAS_2-M_2S-Mg_2S-S$), in which spessartite M_3AS_3 is absent.

Keywords: Manganese ore, agglomerate, dolomite, phase formation, thermodynamic

INTRODUCTION

The ferroalloy industry of Kazakhstan has recently experienced an acute shortage of high-quality manganese ore to produce manganese alloys. Although Kazakhstan has huge reserves of manganese ores, most of them are unsuitable for smelting standard grades of manganese alloys since about 70% are ferromanganese, and 30% are considered difficult to enrich. Unlike manganese ores of the CIS countries, Kazakhstani ores are distinguished by a virtual absence of phosphorus [1, 2]. The manganese ore industry of Kazakhstan needs ferroalloy plants for manganese ore. The share of small classes (less than 10 mm) in manganese ores of Kazakhstan and other countries is 30 - 50% [3-6]. Their use in metallurgical processing is difficult and increases energy costs. In addition, the finely dispersed part of the charge is removed from the furnace units and rotates in the technological cycle, overloading the gas cleaning facilities. During the extraction of manganese ores and at mining and processing plants, many small classes are also formed due to crushing, sorting, flotation, etc. Therefore, many small ores are practically unsuitable for direct use in production processes that require special preparation [7-15]. When processing manganese ores of Kazakhstan using conventional technologies for silicomanganese, the possibility of forming low-melting intermediate, and in some cases even primary slags, additionally characterized by very low viscosity and high electrical conductivity, is inevitable [16]. This is evidenced by extensive studies of the phase composition and state diagrams of multicomponent systems based on iron and manganese oxides conducted at the Chemical and Metallurgical Institute. The phase structure diagrams of the $FeO-MnO-CaO-Al_2O_3-SiO_2$ and $MgO-MnO-CaO-Al_2O_3-SiO_2$ systems have been sufficiently studied previously and described in detail in [17]. Moreover, the first diagram is preferable to use for characterizing manganese ores. It concentrates directly on primary slags from the production of manganese alloys, and the second describes the phase compositions of the final slags.

MATERIAL AND METHODS

Based on the phase structure diagrams of the $FeO-MnO-CaO-Al_2O_3-SiO_2$ and $MgO-MnO-CaO-Al_2O_3-SiO_2$ systems, the standard phase compositions of manganese ores and concentrates from various deposits were calculated, the chemical compositions of which are presented in **Table 1**.

Table 1 Chemical composition of manganese ores and concentrates

Materials	MgO	FeO	MnO	CaO	Al_2O_3	SiO_2
Manganese ores of Kazakhstan from various deposits						
Ushkatyn-III (oxidized ore)	0.73	10.84	52.31	1.69	4.66	10.06
Ushkatyn-III (primary ore)	1.35	6.34	49.14	12.77	1.23	12.63
Eastern Kamys	0.88	3.08	48.41	1.69	3.12	22.10
Manganese ore from the "Tur" deposit						
Lump ore 10-150 mm	0.67	5.57	53.70	1.65	5.14	17.80
Lump ore 40-150 mm	1.89	7.11	53.01	2.30	5.66	18.17
Lump ore 10-40 mm	1.33	8.44	48.58	1.86	5.22	21.30
Ore fine 0-5 mm	1.05	8.96	19.49	1.25	6.49	44.20
Fine ore 0-10 mm	0.88	6.90	25.43	1.33	6.64	37.20

To use the results of thermodynamic-diagram analysis about the studied raw materials, first of all, it is necessary to find those elementary pentatopes in which primary slags are formed and determine the direction of change in their compositions as various fluxing additives are added. Then, focusing on the location of these ores in a particular pentatope, as well as on the standard distribution of their main components between the compounds (secondary phases) located at the tops of a given pentatope, it is possible to provide a metallurgical assessment of the ores and charges based on them. For this, the material compositions of individual grades of manganese raw materials of Kazakhstan were recalculated for five oxides of the F-M-C-A-S system, after which their positions in the factor space of this system were determined with the calculation of the standard number of secondary phases in the corresponding pentatopes. The calculation results are presented in **Table 2**, based on which are studied the properties of manganese ores and concentrates from the Tur deposit in comparison with ores from various deposits in Kazakhstan and developed appropriate technological recommendations for their effective preparation for

metallurgical processing at the stage of their agglomeration using the agglomeration method.

RESULTS AND DISCUSSION

Manganese ores of the "Tur" deposit are classified as low-melting by their temperature characteristics (softening and melting temperatures). This is because, according to their standard phase composition, they are located in the area of pentatope No. 16 (**Fig. 1** and **Fig. 2**) of the phase diagram of the FeO-MnO-CaO-Al_2O_3-SiO_2 system, especially closer to tephroite ($2MnO·SiO_2$). This manganese compound is low-melting and has very high electrical conductivity. Therefore, the smelting process of these ores can be accompanied by the formation of low-melting slags, i.e. the rate of slag formation is higher than the rate of manganese reduction. In the diagram (**Fig. 1** and **Fig. 2**), this compound is designated as Mn_2S. This compound leads to a breakdown in the furnace operation if special measures are not taken to prevent the indicated negative factors [2,3].
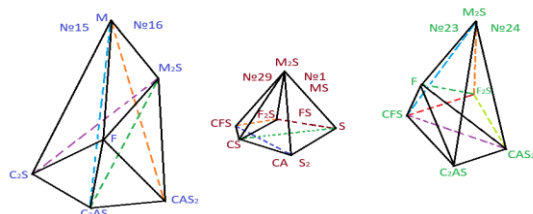

Fig. 1 Sequence of transformation of secondary phases in melts of the FeO-MnO-CaO-Al_2O_3-SiO_2 system
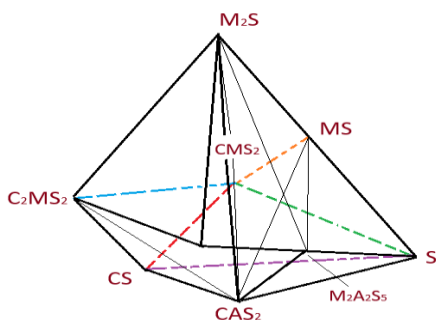

Fig. 2 Magnesia slags of silicomanganese
(phase composition diagrams of the MgO-CaO- Al_2O_3-SiO_2 system)

At the same time, almost all Kazakhstan's manganese ores, including high-silica, carbonate concentrates and ores, are located in pentatopes No. 12; 15 of the F-M-C-A-S system by chemical composition. Consequently, the latter's features determine the characteristics of these materials and the properties of primary slags during agglomeration. If we divide the specified materials by grades, then highly basic manganese ores and concentrates (for example, Ushkatyn-III primary), as a rule, fall into pentatope No. 15 by composition (Table 2), the analytical expressions of the secondary phases of which have the following form:

$$F = F_0 \qquad\qquad C_2AS = 2{,}688A_0$$

$$M = M_0{-}2{,}367S_0 + 1{,}269C_0 \qquad\qquad C_2S = {-}1{,}688A_0 + 1{,}536C_0$$

$$M_2S = 3{,}367S_0 - 1{,}805C_0.$$

In this case, due to the presence of CaO, most of the SiO_2 binds to it, and the proportion of manganosite in them begins to grow (Table 2). Similarly, we can consider the behavior of manganese raw materials located in pentatope No. 12. As follows from expressions (1), as a result of deterioration in the quality of the material (a decrease in the manganese content and an increase in the content of silica and alumina), its composition moves from pentatope No. 15 to the space of F-M-C-A-S systems. The raw material will end up in pentatope No. 12 (the CAS_2 vertex appears) (Table 2).

The standard quantities of secondary phases are calculated using the expressions:

$$F = F_0 \qquad\qquad CAS_2 = 5{,}43A_0{-}4{,}94C_0,$$

$$Mn = {-}2{,}367S_0 - 0{,}696A_0 + 6{,}358C_0{+}Mn_0 \qquad\qquad MA = 1{,}696A_0 - 3{,}097C_0$$

$$M_2S = 3{,}367S_0 - 7{,}236A_0.$$

High-quality ores are strongly shifted in composition toward the manganosite apex of pentatope No. 12, resulting in a significant portion of manganese oxide in the melts in a free state (**Table 2**). This explains the better reducibility of such materials. On the other hand, they must be refractory from the position of the latter's composition in the pentatope. According to data [18], high-quality ores (more than 45% Mn) begin to melt at 1590-1650 K and have a liquidus temperature of 1780-1890 K, which is much higher than the temperature at which Mn starts to be reduced by carbon (1461 K), which corresponds to the data in Table 2. Consequently, the above circumstances, both in thermodynamic and kinetic terms, favor the reduction of manganese during the smelting of silicomanganese. Concentrates from the ores of the Tur and Vostochny Kamys deposits, by composition, are located in pentatope No. 12 and tend to the top of the low-melting (1618 K) tephroite (M_2S) (Table 2). The specified shift in the ore composition causes a decrease in the melting temperature of the ores, a decrease in free manganosite in the melts and an increase in the proportion of manganese silicates. All this directly affects the melting indicators of silicomanganese when using these materials. As noted above, manganese concentrates from the Tur deposit by temperature characteristics (softening and melting temperatures) belong to low-melting ones [19]. This is especially true for screenings of manganese ores from the Tur deposit of fractions 0-5 and 0-10 mm, characterized by a high silica content and, accordingly, a low manganese content. This is because, according to the standard phase composition, they are located in the area of pentatope No. 3 of the phase diagram of the F-M-C-A-S system, closer to the tephroite junction ($2MnO·SiO_2$), which has a low melting point ($t_{melt} = 1345$ ºC) and high electrical conductivity, as well as even more fusible spessartite M_3AS_3 ($t_{melt} = 1205$ ºC). Therefore, it is expected that the smelting process of these ores may be accompanied by the formation of fusible slags, which will lead to the advance of the process of liquid slag formation over the processes of manganese recovery. This will lead to a breakdown in the operation of the furnace if special measures are not taken to prevent these negative factors. This circumstance currently does not allow for the capacity of the furnaces to be raised in workshop No. 1 of the Aksu Ferroalloy Plant, where all the furnaces operate at approximately 60% of the rated capacity of the furnace transformers. To neutralize these negative factors and select the optimal compositions of the batches for smelting silicomanganese, the works [20] propose to move the compositions of the batches to the tephroite-anorthite-gehlenite, tephroite-anorthite-silica planes of the indicated systems.

Table 2 Material and normative phase states of manganese ores and concentrates based on the FeO-MnO-CaO-Al$_2$O$_3$-SiO$_2$ system

| Material	№ pent	Material composition, %					Normative phase composition, %										
		FeO	MnO	CaO	Al$_2$O$_3$	SiO$_2$	CAS$_2$	Mn$_2$S	Mn$_3$AS$_3$	F	M	MA	C$_2$AS	C$_2$S	CMS	S	F$_2$S
Manganese ores of Kazakhstan from various deposits																	
Ushkatyn-III, oxidized	12	13.62	65.75	5.86	2.12	12.64	10.54	27.23	-	13.62	45.22	3.37	-	-	-	-	-
Ushkatyn-III, primary	15	7.72	59.85	15.55	1.50	15.38	-	-	-	7.72	43.20	-	4.03	1.23	43.82	-	-
Eastern Kamys	12	3.93	61.75	2.16	3.98	28.19	10.72	79.31	-	3.93	5.96	0.07	-	-	-	-	-
Manganese ore from the "Tur" deposit																	
Lump ore 10-150 mm	12	6.64	64.04	1.97	6.13	21.23	9.79	57.23	-	6.64	22.04	4.30	-	-	-	-	-
Lump ore 10-150 mm	12	7.10	67.04	0.70	5.69	19.47	3.47	60.52	-	7.10	21.42	7.48	-	-	-	-	-
Lump ore 40-150 mm	12	8.24	61.46	2.67	6.56	21.07	13.27	51.63	-	8.24	23.98	2.87	-	-	-	-	-
Lump ore 10-40 mm	12	9.88	56.89	2.18	6.11	24.94	10.84	68.22	-	9.88	7.44	3.62	-	-	-	-	-
Ore screening 0-5 mm	3	11.15	24.25	1.55	8.07	54.98	7.74	18.95	25.41	-	-	-	-	-	-	32.12	15.79
Ore screening 0-10 mm	3	8.91	32.81	1.72	8.57	48.00	8.54	30.54	26.38	-	-	-	-	-	-	21.93	12.62

When high-alumina slags of anorthite composition are formed, they are viscous, but by adding magnesia, the composition of the final slag can be shifted towards diopside CaO.MgO.2SiO2 to achieve the desired viscosity properties of the slags. When creating a technology for agglomerating manganese raw materials from the "Tur" deposit, these factors must be considered, and the optimal level of magnesia additive must be found (**Table 3**).

When developing an optimal technology for agglomerating high-siliceous manganese ores from the "Tur" deposit, increasing the melting temperature of the agglomerated raw material is necessary to ensure effective smelting parameters. Enough of the binding liquid phase must be obtained to obtain a strong agglomerate, which can be achieved by finding the required level of fuel consumption.
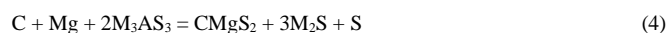
Table 3 Change in the chemical composition of the sinter batch based on manganese ore "Tur" with the introduction of dolomite from 0-15% (calculated)

The amount of dolomite in the charge, %	Chemical composition of sinter batch						
	MgO	FeO	MnO	CaO	Al$_2$O$_3$	SiO$_2$	Sum
0	0.88	6.90	25.43	1.33	6.64	37.20	78.39
1	1.09	6.84	25.18	1.61	6.58	36.83	78.13
2	1.29	6.78	24.92	1.90	6.53	36.46	77.88
3	1.50	6.72	24.67	2.18	6.47	36.10	77.63
4	1.70	6.66	24.41	2.46	6.41	35.73	77.37
5	1.91	6.59	24.16	2.74	6.36	35.36	77.12
6	2.11	6.53	23.91	3.03	6.30	34.99	76.87
7	2.32	6.47	23.65	3.31	6.25	34.62	76.62
8	2.52	6.41	23.40	3.59	6.19	34.26	76.36
9	2.73	6.35	23.14	3.87	6.13	33.89	76.11
10	2.93	6.28	22.89	4.16	6.08	33.52	75.86
11	3.14	6.22	22.63	4.44	6.02	33.15	75.60
12	3.34	6.16	22.38	4.72	5.96	32.78	75.35
13	3.55	6.10	22.12	5.01	5.91	32.42	75.10
14	3.75	6.04	21.87	5.29	5.85	32.05	74.85
15	3.96	5.97	21.62	5.57	5.79	31.68	74.59

Magnesium oxide, in the form of dolomite, is traditionally used to increase the melting point of agglomerated materials. However, it is necessary to consider the effect of dolomite additives on the viscosity of the slag, additional energy consumption for the decomposition of carbonates and the number of liquid phases formed to obtain a strong sinter. To find the optimal dolomite consumption that provides favorable conditions for obtaining agglomerate and its further processing, an analysis was made of the effect of dolomite additives in the composition of the agglomeration batch on changing the chemical (table 3) and phase composition of the agglomerate based on the phase structure diagram of the Mg-M-C-A-S system (**Table 4**). The study of phase formation in the process of agglomeration of manganese ores of the "Tur" deposit when introducing dolomite into the agglomeration batch from the standpoint of thermodynamic-diagrammatic analysis of the Mg-M-C-A-S system shows that the phase composition of substances changes in a certain sequence with entry into one or another pentatope depending on the completeness of the interaction of dolomite and manganese ore. Knowing the initial location in the space of the Mg-M-C-A-S system of the original materials (manganese ore and dolomite), it is easy to trace the dynamics of changes in phase equilibria in the composition of the agglomeration batch, occurring in the process of sintering during agglomeration (**Fig. 2**).
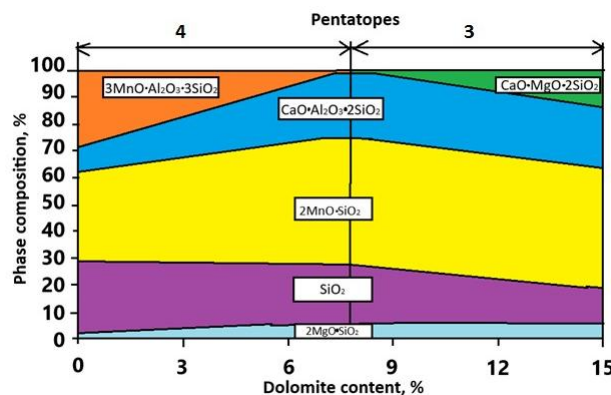
Fig. 3 Dynamics of changes in phase equilibria in the composition of agglomerate when introducing dolomite into the composition of the agglomerate batch

As can be seen from **Fig. 2**, as manganese ore interacts with dolomite in the sinter batch, new phases are formed according to the following reactions:

$$S + C + 2M_3AS_3 = 3M_2S + 2CAS_2, \tag{3}$$

$$C + Mg + 2M_3AS_3 = CMgS_2 + 3M_2S + S \tag{4}$$

$$2Mg + S = Mg_2S, \tag{5}$$

$$C + Mg + 2S = CMgS_2, \tag{6}$$

The addition of dolomite leads to the formation of more refractory compounds. The low-melting compound in the system is spessartite (t_{melt}=1205 ºC) and free silica present in manganese ore screenings when interacting with dolomite, will form more refractory compounds of forsterite Mg_2S (t_{melt}=1860 ºC) and diopside CMS_2 (t_{melt}=1391.5 ºC) according to reactions (3) - (6). As a result, when adding dolomite to the sinter batch of more than 8%, the composition of the agglomerate changes from pentatope No. 4 (M_3AS_3-CAS_2-M_2S-Mg_2S-S) to pentatope No. 3 (CMS_2-CAS_2-M_2S-Mg_2S-S), in which spessartite M_3AS_3 is absent

Table 4 Change in the material and standard phase state of the composition of the sinter batch based on manganese ore from the "Tur" deposit, fraction 0-10 mm, with the introduction of dolomite from 0-15% based on the MgO-MnO-CaO-Al₂O₃-SiO₂ system

The amount of dolomite in the charge, %	№ pent.	Material composition, %					Normative phase composition, %					
		MgO	MnO	CaO	Al₂O₃	SiO₂	CMgS₂	CAS₂	M₂S	M₃AS₃	S	Mg₂S
0	4	1.23	35.58	1.86	9.29	52.04	-	9.41	33.25	28.43	26.82	2.09
1	4	1.52	35.32	2.26	9.23	51.66	-	11.39	35.27	24.43	26.30	2.61
2	4	1.81	35.05	2.67	9.18	51.29	-	13.37	36.99	20.91	25.59	3.14
3	4	2.11	34.79	3.07	9.13	50.91	-	15.35	39.16	16.91	24.92	3.66
4	4	2.41	34.52	3.48	9.07	50.52	-	17.33	40.88	13.39	24.21	4.19
5	4	2.70	34.26	3.89	9.02	50.14	-	19.31	43.05	9.39	23.54	4.71
6	4	3.00	33.99	4.30	8.96	49.75	-	21.29	44.77	5.87	22.83	5.24
7	4	3.30	33.72	4.72	8.90	49.36	-	23.27	46.80	1.86	22.31	5.76
8	3	3.60	33.45	5.13	8.85	48.97	0.72	24.32	47.51	-	21.40	6.05
9	3	3.91	33.17	5.55	8.79	48.58	2.48	24.04	47.23	-	20.25	6.00
10	3	4.21	32.90	5.98	8.73	48.18	4.63	23.77	46.80	-	18.97	5.83
11	3	4.52	32.62	6.40	8.68	47.78	6.17	23.77	46.37	-	17.84	5.85
12	3	4.83	32.34	6.83	8.62	47.38	7.93	23.50	49.09	-	16.68	5.80
13	3	5.14	32.06	7.25	8.56	46.98	9.47	23.50	45.66	-	15.54	5.83
14	3	5.45	31.78	7.68	8.50	46.57	11.62	23.22	45.24	-	14.27	5.65
15	3	5.77	31.50	8.12	8.44	46.17	13.37	22.95	44.81	-	13.09	5.78

Introducing more than 8% dolomite into the sinter batch completely removes the most low-melting compound spessartite from its composition, which should increase the agglomerate's melting point. However, the formation of low-melting tephroite M_2S (t_{melt} = 1345 ºC) in significant quantities (up to 40-50% by weight) according to reactions (3) and (4) can lead, on the contrary, to a decrease in the melting point of the resulting agglomerate. Therefore, we analyzed the effect of introducing dolomite into the composition of the agglomeration batch on its melting point, which was calculated additively based on the phase composition of the agglomeration batch given in Table 4. Although the calculation results shown in Figure 3 are very approximate and do not reflect the true picture of all the processes occurring during melting, they can be used as a first approximation to assess the direction of change in the characteristics of the materials under study when their composition changes.
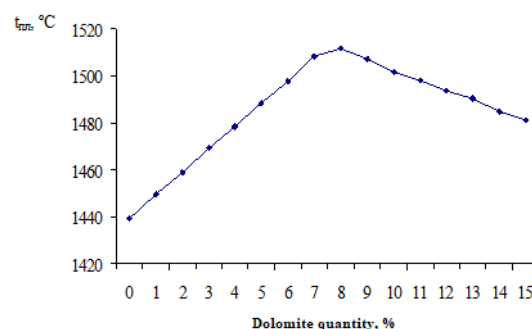
Fig. 4 Effect of the amount of dolomite added to the sinter batch composition on the melting temperature of the sinter

Thus, the assumptions made based on thermodynamic-diagram analysis about the increase in the melting temperature of the sinter batch when introducing dolomite into its composition are confirmed. Introducing dolomite up to 8% leads to a rise in the melting temperature. A further increase in dolomite can lead to a decrease in the melting temperature. The conducted theoretical study on the establishment of phase equilibria in the $MgO-MnO-CaO-Al_2O_3-SiO_2$ system showed that during the agglomeration of manganese ores with dolomite additives, as the high-temperature sintering process proceeds, more refractory compounds of forsterite Mg2S (t_{melt} = 1860 ºC) and diopside CMS_2 (t_{melt} = 1391.5 ºC) are formed. Thus, the nature of the change in the calculated phase composition of the charge materials, revealed from the position of the diagrams constructed in works [21, 22], indicates ways to eliminate factors undesirable for manganese ore electrothermy at the stage of ore preparation by the agglomeration method.

CONCLUSION

The addition of 8.4% dolomite results in the formation of more refractory compounds. The most low-melting compound in the system is spessartite (t_{melt}=1205 ºC) and free silica present in manganese ore screenings, which, when interacting with dolomite, will form more refractory compounds of forsterite Mg2S (t_{melt}=1860 ºC) and diopside CMS_2 (t_{melt}=1391.5 ºC), which results in the transition of the agglomerate composition from pentatope No. 4 (M_3AS_3-CAS_2-M_2S-Mg2S-S) to pentatope No. 3 (CMS_2-CAS_2-M_2S-Mg2S-S), where spessartite M_3AS_3 is absent. The phase structure diagram of the system under consideration, revealed by thermodynamic-diagram analysis, indicates ways to eliminate factors undesirable for manganese ore electrothermy at the stage of ore preparation by the agglomeration method and goal to establish the dynamics of phase equilibria change in the composition of the agglomerate charge during sintering, occurring with the formation of intermediate phases: forsterite Mg_2S and diopside CMS_2. The conducted assessment of the effect of magnesium oxide on the physicochemical properties and phase composition of the resulting agglomerates made it possible to determine the optimal amount of dolomite consumption and improves the technical and economic indicators of smelting manganese alloys. This will have a positive effect on reducing the cost of production processes.

REFERENCES

1. B.A. Svyatov, M.Zh. Tolymbekov, S.O. Baisanov: *Stanovlenie i razvitie margantsevoi otrasli Kazakhstana* (*Development of Kazakhstan's Manganese Industry*), Almaty: Iskander, 2002, 416 p.
2. T. Zhuniskaliyev, Y. Kyatbay, Y. Mukhambetgaliyev, G. Kusainova, A. Abdirashit: Acta Metallurgica Slovaca, 30(3), 2024, 137–141. https://doi.org/10.36547/ams.30.3.2074.
3. A. Zhunusov, L. Tolymbekova, Ye. Abdulabekov, Zh. Zholdubayeva, P. Bykov: Metallurgija, (2021) 60 (1-2) 101-103. https://hrcak.srce.hr/246100.
4. V. Singh, T. Chakraborty, S. Tripathy: Mineral Processing and Extractive Metallurgy Review, 41(6), 2020, 417-438. https://doi.org/10.1080/08827508.2019.1634567.
5. B. Liu, Y. Zhang, M. Lu, Z. Su, G. Li, T. Jiang. Extraction and separation of manganese and iron from ferrugi-nous manganese ores. A review. Minerals Engineering, 131, 2019, 286-303. https://doi.org/10.1016/j.mineng.2018.11.016.
6. V.Ya. Dashevskii, A.A. Aleksandrov, V.I. Zhuchkov, L.I. Leont'ev: Ferrous Metallurgy, 63(8), 2020, 579-590. https://doi.org/10.17073/0368-0797-2020-8-579-590.
7. G.L. Faria, J.A.S. Tenório, Jr. Jannotti, F.G. Araújo: International Journal of Mineral Processing, 137, 2015, 59-63. https://doi.org/10.1016/j.minpro.2015.03.003.
8. Z. Yuanbo, L. Bingbing, Y. Zhixiong, S. Zijian, L. Wei, L. Guanghui: Mineral Processing and Extractive Metallurgy Review, 37(5), 2016, 333-341. https://doi.org/10.1080/08827508.2016.1218870.
9. Ch.Alireza, B. Hanka, E. Hosna, Y. deh Hossein, S. Jafar: Materials Today Communications, 25, 2020, 101382. https://doi.org/10.1016/j.mtcomm.2020.101382.
10. A. Heba, M. El-Sadek, H. Ahmed: Mineral Processing and Extractive Metallurgy, 132(1), 2023, 62-72. https://doi.org/10.1080/25726641.2022.2161736.
11. D. Zhu, T. Chun, J. Pan, J. Zhang: International Journal of Mineral Processing, 125, 2013, 51-60. https://doi.org/10.1016/j.minpro.2013.09.008.
12. A. Kenzhebekova, A. Zhunusova: Science and Technology of Kazakhstan, 4, 2021, 59-66. https://doi.org/10.48081/FIZV7488.
13. A. Zhunussova, P. Bykov, A. Zhunusov, A. Kenzhebekova: Kompleksnoe Ispolzovanie Mineralnogo Syra, 329(2), 2024, 73-81. https://doi.org/10.31643/2024/6445.19.
14. A. Tastanova, S. Temirova, B. Sukurov, A. Biryukova, G. Abdykirova: Processes, 11(12), 2023, 3328. https://doi.org/10.3390/pr11123328.
15. A. Issagulov, N. Ospanov, A. Bayssanov, Y. Makhambetov, D. Issagulova: Metalurgija, 55(4), 2016, 709–711. https://hrcak.srce.hr/file/232016.
16. M.Zh. Tolymbekov, A.B. Akhmetov, S.O. Baisanov, E.A. Ogurtsov, D.M. Zhiembaeva: Steel in Translation, 39, 2009, 416–419. https://doi.org/10.3103/S0967091209050131.
17. M.Zh. Tolymbekov, S.O. Baisanov, O.E. Privalov, L.V. Osipova: Steel in Translation, 38(8), 2008, 654–659. https://doi.org/10.3103/S0967091208080172.
18. S. Gabdullin, S. Baisanov, S. Kim, A. Mukhtar: Metalurgija, 60 (1-2), 2021, 82-84. https://hrcak.srce.hr/file/357480.
19. D. Yessengaliyev, S. Baisanov, A. Issagulov, A. Baisanov, O. Zayakin, A: Abdirashit: Metalurgija. 2019. 58(3-4) 291–294. https://hrcak.srce.hr/218404.
20. M.Zh. Tolymbekov, A.B. Akhmetov, T.D. Takenov: Steel in Translation, 1, 2004, 22–24. https://www.researchgate.net/publication/295295489.
21. M.Zh. Tolymbekov, S.O. Baisanov, O.E. Privalov, L.V. Osipova: Steel in Translation, 38, 2008, 654–659. https://doi.org/10.3103/S0967091208080172.
22. B.A. Svyatov: Steel in Translation, 8, 2002, 55–58. https://www.researchgate.net/publication/292202259.